Antimicrobial metal-organic frameworks incorporated into electrospun fibers

Antimicrobial metal-organic frameworks incorporated into electrospun fibers

Jennifer Quirós[a], Karina Boltes[a], Sonia Aguado[a], Roberto Guzman de Villoria[b], Juan José Vilatela[b] and Roberto Rosal[a,c,*]

[a] Department of Chemical Engineering, University of Alcalá, 28871 Alcalá de Henares, Madrid, Spain
[b] Madrid Institute for Advanced Studies of Materials (IMDEA Materials Institute), Tecnogetafe, E-28906, Madrid, Spain
[c] Madrid Institute for Advanced Studies of Water (IMDEA Agua), Parque Científico Tecnológico, E-28805, Alcalá de Henares, Madrid, Spain

* Corresponding author: roberto.rosal@uah.es

Abstract

The objective of this paper is to present a new class of polylactic acid (PLA) fibers containing cobalt-based metal organic frameworks (MOF). The material used was Co-SIM-1, a cobalt-based substituted imidazolate. Composite mats were prepared by electrospinning PLA with a suspension of polyvinylpyrrolidone-stabilized Co-SIM-1. MOF particles formed aggregate of a small number of primary particles that, after electrospun, became completely embedded inside polymeric fibers. The dispersion of particles was better for lower loadings, for which the relative amount of metal released to culture media was also higher. The antimicrobial activity of composite mats was assessed using SEM images, fluorescence microscopy, direct plate reading of fluorescent stains and plate count of colony forming units among other. The microorganisms used in this study were *Pseudomonas putida* and *Staphylococcus aureus*. Fluorescence techniques allowed recording viable and damaged cells directly on mat surface and in the culture media embedding the fibers. The results showed higher sensitivity of *S. aureus* to cobalt-containing fibers, with a reduction in colony forming units of up to 60% with respect to PLA mats. The results also showed the presence of viable but non-culturable microorganisms, which fail to form colonies but yield a positive signal to viable cell staining. Cobalt-based MOF included in electrospun mats provide antibacterial activity suitable to be used to prepare membranes for various biomedical applications.

Keywords: Electrospinning, Polylactic acid, Cobalt, Metal–organic frameworks, Microbiocidal fibers.

1. Introduction

Metal–organic frameworks (MOF) are a remarkable class of materials in which organic bridging ligands are connected by metal ions to form one-, two-, and three dimensional coordination networks [1]. The key advantages of MOF compared to inorganic microporous structures such as zeolites, is their highly tunable composition, which can be achieved by using different metals or changing the organic linker. The initial interest on MOF came from their very high surface areas and hence an extremely high capacity to capture gases in energy-related technologies [2,3]. Many other potential applications have been proposed for MOF in fields like heterogeneous catalysis, gas purification and sensing [4,5]. The focus on gas-related processes has been recently complemented with novel biological applications based on the capacity of coordination polymers for the controlled release of bioactive molecules, either physisorbed within the pore structure or behaving themselves as linkers in pro-drug form [6]. New developments are increasingly focused on the development of materials of complex chemical functionalization in order to impart tailored chemical and physical properties [7].

The release of metal ions contained in the structure of MOF makes them attractive antimicrobial materials for applications in which a tunable antibiotic is required. Silver ion releasing compounds are a well known family of antimicrobials and several silver containing MOF have been reported up to date to this end. Berchel et al. reported a silver-based MOF with a 3-phosphonobenzoate ligand that acts as a source of silver ions and showed antibacterial activity against Staphylococcus aureus, Escherichia coli and *Pseudomonas aeruginosa* [8]. Liu et al. reported another silver-based metal–organoboron framework with antibacterial activity against Gram-negative and Gram-positive human pathogens [9]. Hindi et al. [10] and Slenters et al. [11] prepared other silver-based coordination compounds with proved or suggested

biocidal capacity. Silver, however, is an expensive metal and the indiscriminate use of it in many consumer goods is suspected to promote not only a general toxic risk but also bacterial resistance [12]. Silver was also incorporated in different types of nanofibers in order to incorporate antimicrobial effect. Sheikh et al. prepared silver doped polyurethane nanofibers via electrospinning in which silver nanoparticles were obtained from silver nitrate by in situ reduction with N,N-dimethylformamide [13]. Shi et al. prepared silver nanoparticle-filled nylon 6 nanofibers by electrospinning, the electrospinning solvent behaving as reducing agent for in situ conversion of $AgNO_3$ into silver nanoparticles [14]. Several groups reported the use of electrospinning to prepare hybrid nanomaterials for antimicrobial applications by loading chitosan-based fibers with silver nanoparticles [15,16].

In a recent paper Aguado et al. reported high antibacterial activity of a cobalt imidazolate MOF [17]. The results showed that the controlled release of cobalt gave rise to a long-lasting antibacterial activity with the advantage with respect to silver that it is a relatively inexpensive element, still active for bacteria but less toxic than silver [18]. Zhuang et al. also proposed a cobalt MOF with tetrakis[(3,5-dicarboxyphenyl)-oxamethyl] methane acid as ligand, which demonstrated activity for the inactivation of *E. coli* [19]. Concerning other metals, Sancet et al. prepared surface-anchored copper MOF with dual functionality, intended to combine sensing and controlled release of an antimicrobial metal ion [20]. The material was tested using the marine bacteria *Cobetia marina*, and displayed good surface response to adhering microorganisms. It is interesting to point out that in most cases, the linker used in the preparation of MOF reservoirs was not commercially available, the synthesis of it requiring several reaction-separation steps. In this work, we tested a cobalt-based MOF prepared using a simple, relatively cheap and commercially available ligand [21].

Electrospinning is a simple method for generating nanofibers from a wide variety of materials, including many dissolved or melted polymers, using a high-voltage power supply. Electrospun fibers have been proven useful in a number of fields such as water filtration, the design of sensors, the manufacturing of special clothing and many biomedical applications such as wound dressings or scaffolds for tissue engineering [21,22]. Electrospun fibers have attracted considerable attention due to their remarkable properties, which include small diameter and relatively high surface-to-volume ratio, even though the preparation of porous polymer nanofibers with high surface areas is still a challenge [23]. The incorporation of particles into electrospun polymer nanofibers has also been explored by researchers working in drug delivery applications and in water treatment technologies [24,25].

The purpose of this study was to prepare and test a biocidal composite material consisting of a cobalt-based MOF embedded in an electrospun polymeric matrix based on polylactic acid (PLA). PLA is derived from renewable resources and displays higher natural hydrophilicity than conventional thermoplastic polymers as a result of better access of water to the polar oxygen linkages in the backbone. This fact has been shown to improve water fluxes and reduce the biofouling tendency of membranes made of PLA [26]. PLA also displays a good spinnability. The composite Co-–MOF-–PLA material is intended for use in antimicrobial applications such as the preparation of antibacterial tissues or the production of membranes for water treatment.

2. Materials and methods

2.1 Materials

Transparent PLA (trade name: ‘PLA Polymer 2002D’) was purchased in the form of pellets from NatureWorks LLC, UK with a melt index of 5–7 g/10 min (at 210 °C/2.16 kg), a molecular weight of ~121,400 g/mol, a melting temperature of 160 °C and a d-content of 4% (96% l-lactide content). Polyvinylpyrrolidone (PVP), molecular weight 360,000 from Sigma–Aldrich was used as dispersant. Dichloromethane (DCM, 99.5%), used as solvent for PLA, and acetone (99.8%) were reagent grade, obtained from Sigma–Aldrich and used as received. The components of culture media were biological grade reagents acquired from Conda-Pronadisa (Spain). Fluorescein diacetate (FDA, CAS Number 25535-16-4) and propidium iodide (PI, CAS Number 596-09-8) acquired from Sigma–Aldrich were used as cell viability stains. Live/Dead BacLight Bacterial Viability Kit was acquired from Molecular Probes.

Co-SIM-1 (cobalt-based Substituted Imidazolate Material) is a novel analogue of its zinc-based parent SIM-1 [27,28]. It consists of CoN_4 tetrahedra linked by methyl-carboxyaldehyde-imidazolate, belongs to the class of ZIF or ZMOF materials and is isostructural to ZIF-8 and ZIF-67. Co-SIM-1 was synthesized by solvothermal procedure reported elsewhere [17,27,29]. Briefly, 0.199 g (0.68 mmol) of $Co(NO_3)_2 \cdot 6H_2O$ and 0.301 g (2.7 mmol) of 4-methyl-5-carboxyaldehyde-imidazole were dissolved in 5 mL of DMF, the resulting solution being heated to 358 K for 72 h. The resulting powder was washed three times with DMF and then with ethanol and dried at 373 K overnight.

2.2 Electrospinning

A NANON-01A electrospinning unit (Mechanics Electronic Computer Corporation, MECC Co., Ltd., Japan) was used to prepare composite mats. 7 wt.% PLA solution was prepared by dissolving the required amount of PLA pellets in DCM under constant magnetic stirring for 24 h. Co-SIM-1 was dispersed in a 2.5 wt.% PVP solution in DCM by mechanical stirring followed by sonication for 3 min in pulsed mode (30 s pulses with 30 s delay after every pulse in order to avoid sample overheating) using an ultrasonic processor VC505 (500 W, 20%) from Sonics & Materials Inc. The concentration of dispersed particles was typically 30% over the desired

final concentration in the mat. Subsequently, Co-SIM-1dispersion and PLA solution were mixed at 1:1 ratio. Co-SIM-1 loadings were 2, 4.5 and 6 wt.% of the final weight of electrospun composite mats. (From ICP measurements, the true Co-SIM-1 content of the electrospun fibers used in this work was 2.06 ± 0.07, 4.63 ± 0.17 and 6.04 ± 0.10.) After vigorous magnetic stirring the resulting dispersion fed the electrospinning machine with the following parameters: voltage ~21 kV; feed rate ~0.9 mL/h; distance between the tip of the needle and drum collector ~15 cm; and drum rotation speed ~500 rpm.

2.3 Analytical methods

The morphology of fibers after was examined using a scanning electron microscope (SEM) from Carl Zeiss (EVO MA15) at an accelerating voltage of 18 kV and probe intensity of 120 pA. A process of dehydration and drying with acetone and ethanol was carried out to analyze mats in contact with microorganisms by SEM. The morphology of pristine and composite mats was also investigated using atomic force microscope (AFM) using a Park NX10 equipment in non-contact mode. X-ray diffraction (XRD) measurements were recorded in the 10–90° 2θ range (scan speed = 20 s, step = 0.04°) by powder XRD using a Shimadzu 600 Series Diffractometer employing CuKα radiation (λ = 1.5418 Å). The zeta potential of Co-SIM-1 particles was obtained using electrophoretic light scattering combined with phase analysis light scattering in a Malvern Zetasizer Nano apparatus. The measurements were conducted at 25 °C and pH 7.0 using 10 mM KCl water or the culture medium as dispersants. The size distribution of particles (< 6000 nm) was obtained using dynamic light scattering (DLS) using the same instrument. Inductively Coupled Plasma-Mass Spectrometry analyses (ICP-MS) were performed on a NexION 300XX de Perkin-Elmer. Optical density was measured at 600 nm using a Shimadzu UV Spectrophotometer UV-1800.

2.3 Microbial bioassays

The microorganisms used in this study were *Pseudomonas putida* (ATCC 12633) and *Staphylococcus aureus* (ATCC 6538P). The microorganisms were maintained at −80 °C in glycerol (50% v/v) until use. Reactivation was performed by culture in 50 mL Erlenmeyer's flask and tracked by measuring optical density (OD) at 600 nm. Microorganisms were grown at 30 °C, 150 rpm during 24 h to reach stationary phase. The culture medium used was, for 1 L solution in distilled water, beef extract 5 g, peptone 10 g, NaCl 5 g and, for solid media, agar powder 15 g. The pH was adjusted to 7.2.

Bacterial viability was assessed using fluorescence microscopy as follows. Cells of *S. aureus* or *P. putida* were incubated overnight for reactivation. Approximately 1×10^4 cells were inoculated and incubated during 24 h on mats containing different amounts of Co-SIM-1 (from 0 to 6 wt.%). Subsequently, the liquid fraction of each culture was separated from mats for independent staining and microscopy observation. A Live/Dead BacLight Bacterial Viability Kit (Molecular Probes, Invitrogen Detection Technologies, Carlsbad, CA, USA) was used to evaluate bacterial viability. In this staining system, viable cells exhibit green fluorescence (SYTO 9), whereas nonviable bacterial cells display red fluorescence (PI) with dye uptake depending upon cell membrane integrity so that dead bacteria can be easily distinguished from viable bacteria. For the staining of cultures, 1 mL of each sample was transferred to an Eppendorf tube and stained with 10 μL of BacLight stain (a mixture of SYTO 9 and PI in DMSO, according to the manufacturer's recommendations). For mat staining, the whole surface of each mat was covered with BacLight stain in a Petri dish, using an amount of 20 μL/cm^2. In both cases the incubation was performed in the dark for 15 min at room temperature. After incubation, 1 μL of each liquid sample or 1 cm^2 of mat was transferred to a glass slide, covered with a glass cover slip and sealed. The results were immediately observed using a Leica Microsystems Confocal SP5 fluorescence microscope. For green fluorescence (SYTO 9, live cells) excitation was performed at 488 nm (Ar) and emission was recorded at 500–575 nm. For red fluorescence (PI, dead cells), the excitation/emission wavelengths were 561 nm (He–Ne) and 570–620 nm respectively. The overlap of green and red appeared yellow.

Bacterial viability was also tested using fluorescein diacetate (FDA), a fluorogenic substrate, which permits the detection of enzymatic activity and PI. The fluorescence was measured in a fluorometer/luminometer Fluoroskan Ascent FL. A plate adapter specifically designed to accommodate two 59 mm Petri dishes was used. For this test, 4 mL of the growth medium diluted to approximately 6×10^8 cell/mL was transferred to a Petri dish in contact with electrospun mats and maintained in a rotary shaker at 150 rpm for 20 h at 30 °C. After incubation, the liquid fraction of cultures was transferred to 96-well microplates by triplicate. A concentration of 0.02% (w/w) in DMSO was used for FDA and PI in all cases. 5 μL of fluorescent stains were added to 195 μL of medium in 96-well plate. For fluorescence reading, after 15 min of incubation at 25 °C, FDA was excited at 485 nm, and emission recorded at 538 nm. PI excitation and emission wavelengths were 530 nm, 645 nm respectively. Concerning mats, 300 μL of the fluorescent stains was carefully extended over the whole mat surface. The Petri dishes with mats were placed inside the Fluoroskan holder. The fluorescence emitted was measured in top mode, using an integration time of 60 ms. This plate reader method permits to obtain 320 data points over each surface as indicated in Fig. S1 (Supplementary information).

Samples from supernatant in contact with mats were taken to carry out a standard plate count. For it 250 μL was inoculated with serial dilutions 1/100 and 1/10 and

incubated for 24 h at 37 °C. A countable plate was considered that containing between 25 and 300 colonies. We also performed digital image analysis of Petri dishes inoculated with microorganisms. Every image was digitally treated to convert it into a B&W image using the public domain Java image processing software ImageJ. Counting black (pixel with colour 0–5) and white (pixels with colour 250–255) pixels yielded the percent area free of bacterial growth.

The disk diffusion method was also used to test the antibacterial behaviour of Co-SIM-1 as described by Driscoll et al. [30]. Petri dishes were prepared with culture media as indicated before, the cellular concentration in inoculums adjusted to OD = 1. 500 μL of each microbial suspension were transferred to plates for inoculation and allowed to dry at room temperature before the addition of antimicrobials. Instead of the standard filter paper disks, 13 mm Whatman anodic alumina discs with Co-SIM-1 deposited on their surface were placed onto the inoculated agar plate. Zone diameters in the disk diffusion assay were measured to the nearest millimeter after 24 h at 37 °C. Control plates were incubated under the same conditions to check correct microbial growth. Sterile plates without inoculation were also incubated to detect possible sample contamination.

3. Results and discussion

3.1Characterization of mats

Cobalt metal–organic Co-SIM-1 was characterized by XRD in order to assess their crystallinity. Fig. S2 (Supplementary information, SI) shows a typical diffractogram, which is good agreement with the corresponding pattern. Fig. S3 (SI) is an image of Co-SIM-1 particles showing that most of them have a primary particle size below 1 μm.

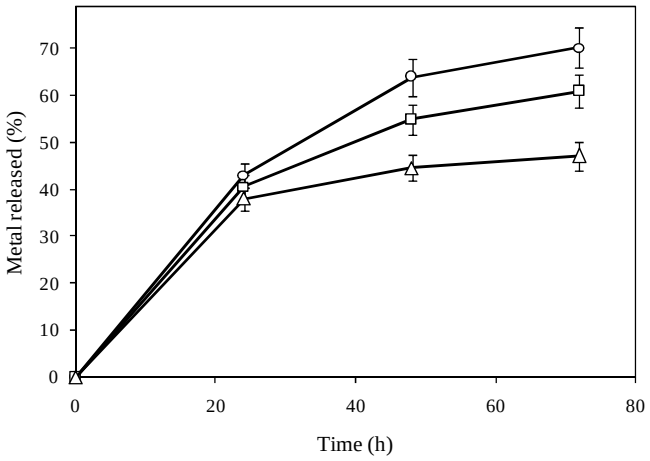

Figure 1. Metal released for mats in contact with culture medium. Co-SIM-1 content in wt. %: 2 % (○), 4.5 % (□) and 6 % (Δ).

Electrospun mats were prepared with three different Co-SIM-1 loadings: 2, 4.5 and 6 wt.%. (A picture of a typical mat is shown in Fig. S1.) The MOF content of electrospun mats was assessed using ICP-MS. ICP-MS was also used to determine the loss of metal in contact with culture media. In all cases the amount of metal released was very similar during the first 24 h, with average cobalt percent loss of 40.6 ± 2.5 (%). The time profile for metal release is displayed in Fig. 1, which also shows that most of it took place during the first 24 h. For mats loaded with a lower amount of Co-SIM-1, the metal was released at a higher rate. This is most probably a consequence of metal diffusion being limited by fiber surface and not by MOF loading.

Most unloaded PLA fibers have diameters in the 1–2 μm range, which is confirmed by SEM (Fig. 2). Fig. 2 shows (A and B) images of neat PLA fibers and (C and D) Co-SIM-1 loaded mats. Co-SIM-1 particles consist of aggregates of several microns formed by up to several tens of primary particles. This is clearly shown in Fig. 2D. The DLS average size of Co-SIM-1 in colloidal suspension in DMF was 274 nm, which is close to the SEM size observed for primary particles. After mechanical redispersion, the DLS size (also in DMF before the final heating during Co-SIM-1 synthesis) increased to 1440 nm, which is somewhat smaller that the size of aggregates embedded in fibers (Fig. 1). The best results for particle dispersion were obtained using 2.5 wt.% PVP as stabilizing agent [31]. The dispersant becomes finally included in PLA mats with 26 wt.% without any evidence of phase segregation or preferential location inside electrospun fibers. AFM images (SI, Fig. S4 A and B) show PLA and PLA loaded with Co-SIM-1 (6 wt.%) with the same results. Both display a non-smooth surface with elongated nanopores of about 50 nm. These structures have been attributed to a fast evaporation of solvent giving rise to local phase separation, so that the solvent-rich zones transformed into cavities or pores during electrospinning [32].

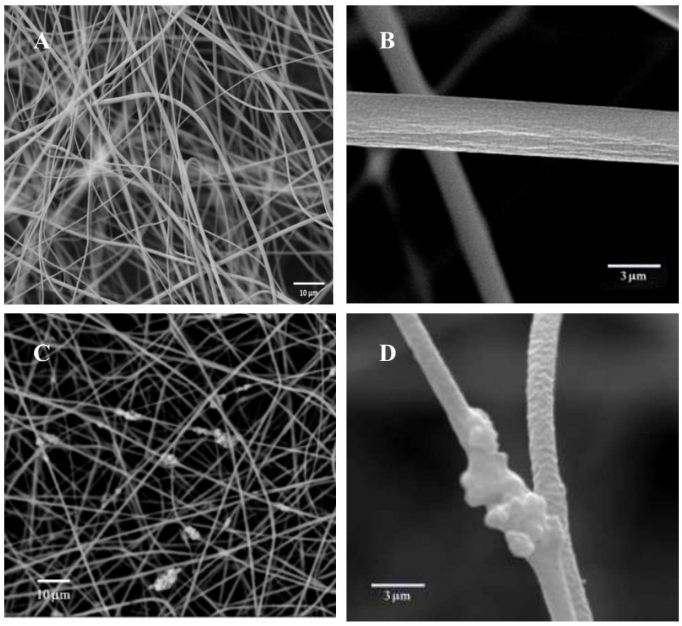

Figure 2. SEM micrographs of (A and B) neat PLA, (C, D) PLA/Co-SIM-1 fibers.

3.2Microbiological growth

Fig. 3 shows SEM micrographs of mats kept in contact for 20 h with cultures of *P. putida* and *S. aureus* and washed before imaging. Pure PLA fibers (A and D), 4.5 wt.% Co-SIM-1 (B and E), 6 wt.% Co-SIM-1 (C and F), A–, B and C corresponding to P. putida and D–, E and F to S. aureus. Biofilm formation can be clearly observed in neat PLA mats as shown in Fig. 3D. Biofilms consist of a single or multiple species of bacteria included in extracellular polymeric substance (EPS) consisting of polysaccharides, proteins, and nucleic acids. *P. putida* is a rod-shaped, flagellated, Gram-negative saprotrophic bacterium found in soil and water habitats. *S. aureus* is a Gram-positive coccal bacterium, which is part of human flora but also a major opportunistic human pathogen. Different species of Pseudomonas and Staphylococcus have been identified as biofilm forming microorganisms in biofouled surfaces such as membranes and medical devices [33,34]. In fact, both genus, Pseudomonas and Staphylococcus, are well known for their biofilm forming ability on most surfaces [35]. For increasing amounts of Co-SIM-1 in fibers it could be observed a clear reduction of bacterial colonization and biofilm growth. Fig. 3C and F corresponds to fibers with 6 wt.% Co-SIM-1, which were reasonably free of microorganisms throughout the fibers, and not only at specific locations such as the thicker parts where MOF aggregates were evident. This fact indicates that cobalt released from fibers passed through the PLA encapsulating MOF and prevented microbial growth in all the environment of loaded mats. In order to get a deeper insight on the effect of Co-SIM-1 on bacteria, we performed a set of microbiological tests using confocal microscopy and several quantitative tests for microbial growth assessment, which are discussed in the following paragraphs.

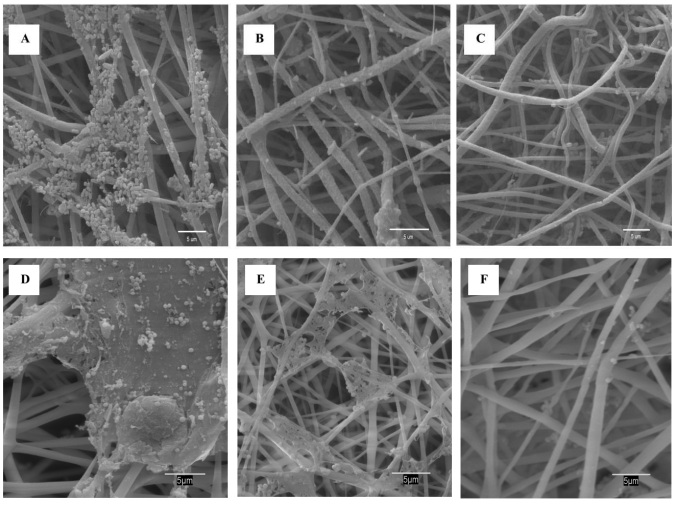

Figure 3. SEM micrographs of fibers in contact (20 h) with cultures of *P. putida* (A, B, C) and *S. aureus* (D, E, F). Pure PLA fibers (A and D), 4.5 wt. % Co-SIM-1 (B and E), 6 wt. % Co-SIM-1 (C and F).

The influence of MOF loaded mats on agar plate coverage was studied using cultures grown for 20 h at 37 °C on agar plates with culture media. Mats, either neat PLA or Co-SIM-1 loaded fibers, were placed on the surface of Petri dishes and allowed to grow. Digital picture processing of Petri dishes allows calculating the percent area free of bacterial growth as shown in Fig. 4. All experiments were replicated until reasonable standard deviation was obtained, which was also indicated in Fig. 4 as error bars. A reasonably linear relationship was obtained between Co-SIM-1 content of fibers and the area that remained optically free of bacterial coverage after the prescribed incubation time of 20 h. For 6 wt.%, up to 30–40% of the surface of mats was clear, with no apparent bacteria coverage either with cultures of *P. putida* or *S. aureus*. The inhibition was slightly higher for *P. putida* but the method did not allow sufficient precision. This point will be addressed to below.

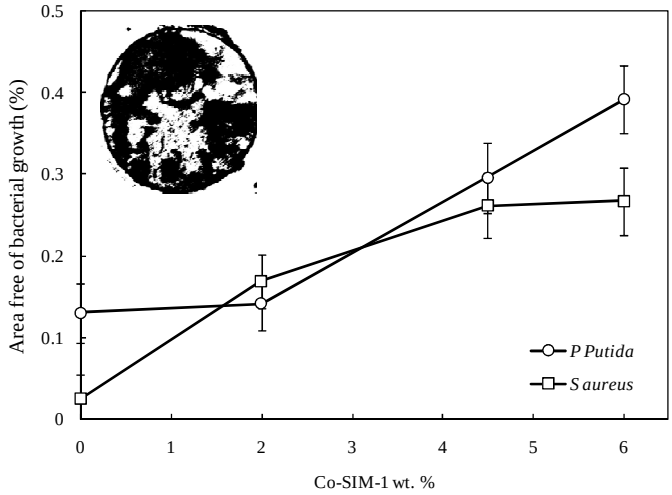

Figure 4. Area free of bacterial growth for mats in contact for 20 h with cultures of *P. putida* (□) and *S. aureus* (□) as a function of Co-SIM-1 content of fibers. Inset: example for P. putida 4.5 wt. % Co-SIM-1 with image digitally treated to display areas free of bacterial growth in white.

The results of Live/Dead BacLight Bacterial Viability Kit on neat and Co-SIM-1-loaded mats are displayed in Figs. 5 and 6. In both cases the micrographs display the double staining (SYTO 9 and PI, green and red respectively) which highlights viable (green) and membrane damaged (red) cells. In both cases, *P. putida* and *S. aureus*, there were no (or very few) damaged cells in pure PLA mats. For increasing amounts of Co-SIM-1 the number of red marked cells increased both in cultures in contact with mats (right) on mat surface itself (left). The effect of the biocidal cobalt compound was more apparent for *P. putida*, particularly when measuring mat surface, which was mostly covered with dead or non-viable cells (Fig. 5D and F). The difference between *S. aureus* and *P. putida* could be attributed to differences in cobalt intake as explained below. The more rapid growth of the later for the experimental conditions used in this work could also play a role. It is interesting to note that the green stain SYTO 9 was also marking (green) individual fibers as shown in Figs. 5 and 6B, D and F. This interference could not be avoided and led to the substitution of SYTO

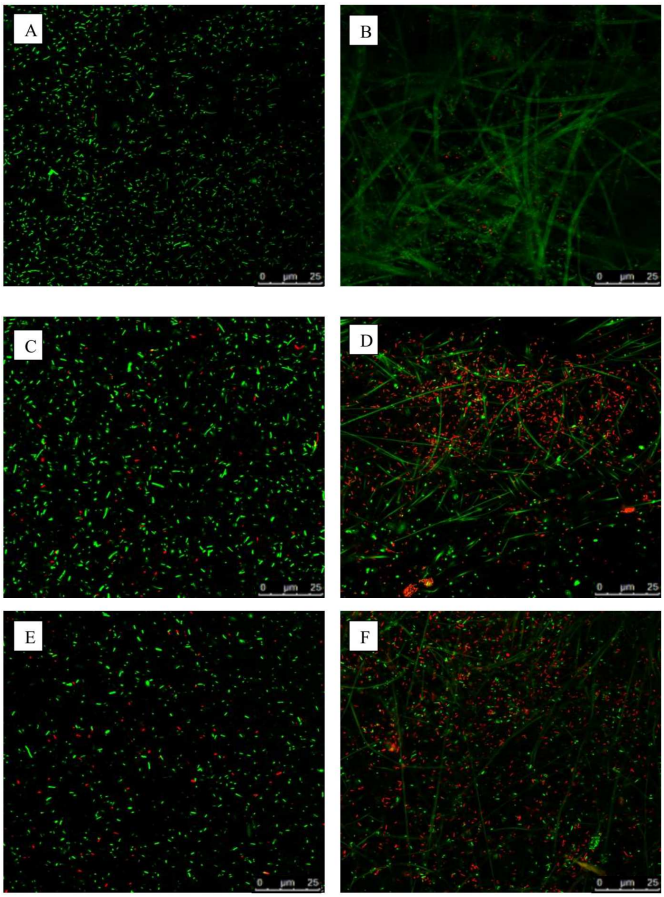

Figure 5. Live/Dead double staining of *P. putida* on mats. A, C and E: cultures in contact with mats; B, D and F: fibers. A and B: neat PLA, C and D: 4.5 wt. % Co-SIM-1, E and F: 6 wt. % Co-SIM.1. Contact time, 20 h.).

9 by FDA in quantitative fluorescence measurements. These were performed using plate luminometer for cultures and for the direct reading of mat surface as described before. The results are shown in Fig. 7 (A for *P. putida* and B for *S. aureus*), which corresponds to data obtained for FDA (viable cells) and the parallel counting of colony forming units (CFU) for cultures kept during 20 h on the surface of mats with different amount of Co-SIM-1. Quantitative data show higher sensitivity of the colony forming capacity of *S. aureus* to the inclusion of cobalt in fibers, with CFU reduction of 60% with respect to neat PLA mats. The results obtained from FDA and CFU followed the same trend and confidence intervals generally overlap, but there is a clear tendency of CFU towards lower values in loaded fibers. This effect may be a consequence of the existence of viable but non-culturable microorganisms (VBNC). It refers to bacteria that fail to grow on the routine bacteriological media on which they would normally grow and form colonies but are alive and with metabolic activity [36]. This phenomenon is often observed in microorganisms under stress conditions such as those induced during disinfection [37]. FDA staining for viable cell counting showed a decrease of up to 30–40% for 6 wt.% Co-SIM-1 mats, which was somewhat larger for *P. putida*. Microplate simultaneous readings of FDA-PI showed coincident results with lower FDA inhibition for *S. aureus*. The signal of PI-stained non-viable cells was considerably larger for *P. putida*, which could be attributed to the different kind of microorganism (Fig. 8). In fact, the internalization to cobalt in Gram-negative bacteria is determined by transenvelope efflux driven by proteins of the resistance-nodulation-cell division group, while for Gram-positive bacteria cobalt is taken up by cation-diffusion facilitator proteins [38]. It is important to note that the counting of viable and non-viable cells was performed in bacterial culture medium and at the most favourable growing conditions for them. A higher inhibition could be expected under conditions less favourable for microbial growth [39].

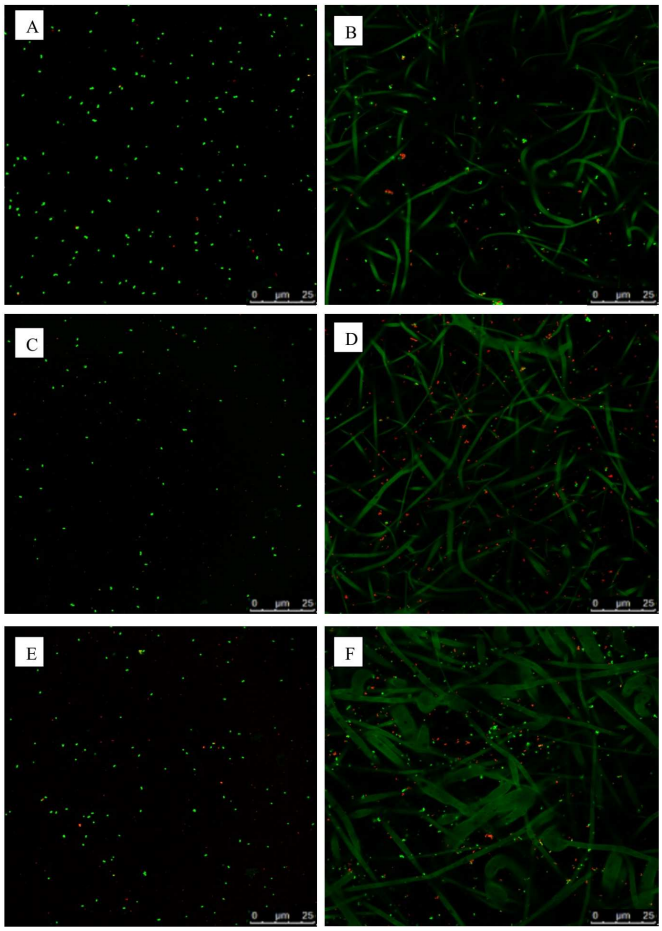

Figure 6. Live/Dead double staining of *S. aureus* on mats. A, C and E: cultures in contact with mats; B, D and F: fibers. A and B: neat PLA, C and D: 4.5 wt. % Co-SIM-1, E and F: 6 wt. % Co-SIM.1. Contact time, 20 h.

The possibility of electrostatic repulsion between Co-SIM-1 nanoparticles and the surface of bacteria was also explored. The surface of bacteria possesses large negatively charged domains due to the presence of anionic glycopolymers or lipopolysaccharides, which could be repelled by negatively charged particles. The zeta potential of Co-SIM-1 particles in water at pH 7 was −11.7 ± 0.7, while in culture medium at the same pH the value was −9.6 ± 0.5. These values can be considered low enough to neglect the possibility that physical repulsion may play any role in keeping the surface of mats free of microorganisms, particularly considering that MOF particles were embedded in a PLA matrix.

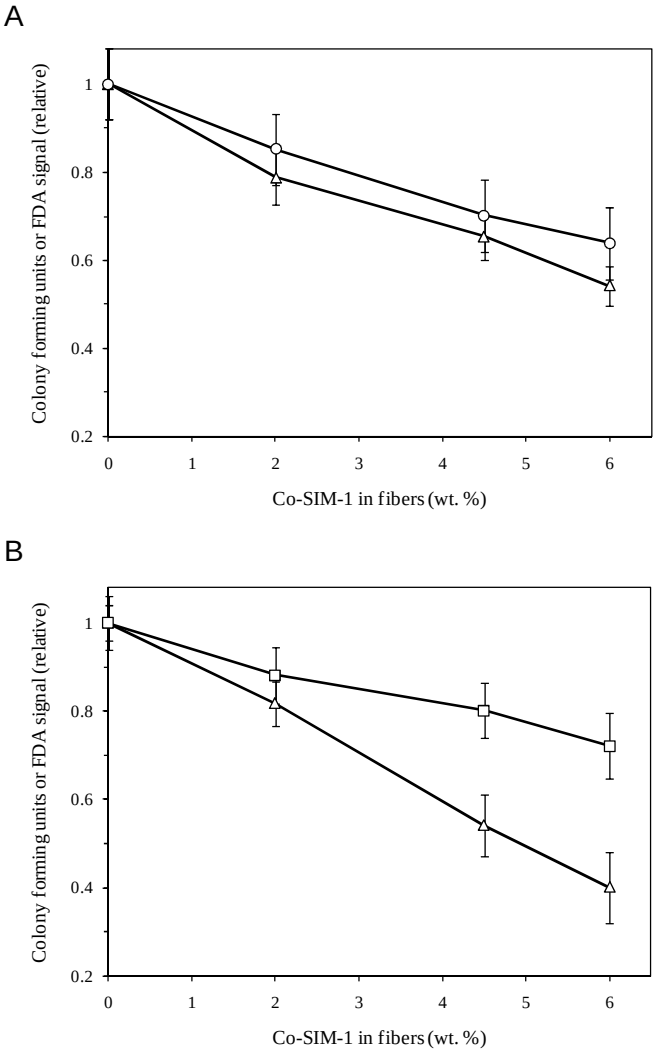

Figure 7. Colony forming units (○, □) and FDA signal (Δ) relative to blank runs for mats electrospun with different amounts of Co-SIM-1. A: P. putida (○), B: *S. aureus* (□).

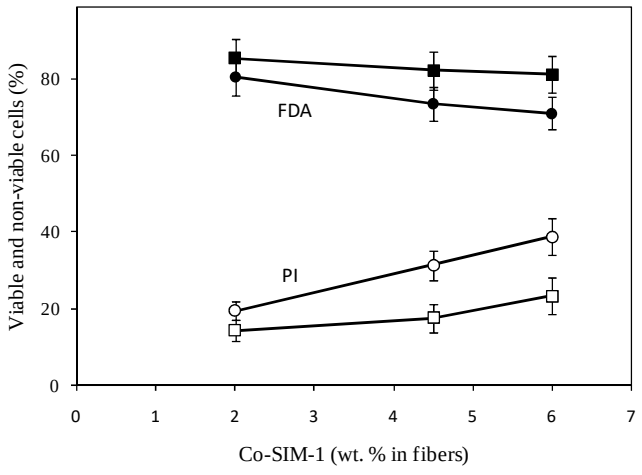

Figure 8. Viable and non-viable cells from FDA and PI staining respectively. *P. putida* (○, •), B: *S. aureus* (□, ■). FDA: filled symbols, PI: empty symbols.

Finally, Fig. S5 shows the inhibition diameter for Co-SIM-1 coated alumina disks after incubation at 37 °C in agar plates previously inoculated with *P. putida* or *S. aureus*. The circles indicate inhibition areas, which were 23.6 ± 1.4 mm for *P. putida* and 25.4 ± 0.801 mm for *S. aureus*. (13 mm was the diameter of alumina discs.) The inhibition diameter was slightly higher for P. putida, although confidence intervals almost overlap. This result is in good agreement with the quantitative data obtained from stained cells and indicates that, Co-SIM-1 biocidal effect is exerted independently of its interaction with PLA or PVP in fibers.

4. Conclusions

A cobalt-based metal–organic framework, Co-SIM-1, was successfully included in a PLA electrospun mat with MOF loadings in the 2–6 wt.% range. The suspension was stabilized during all the electrospinning injection time using a solution of PVP 2.5 wt.%. PLA fibers displayed diameters in the 1–2 μm range in which Co-SIM-1 particles consisted of aggregates of several microns formed by aggregation of some tens of primary particles. All Co-SIM-1 aggregates were completely covered by PLA in composite mats.

SEM images showed that for increasing concentrations of Co-SIM-1, the fibers became less susceptible to bacterial colonization and biofilm formation. Confocal microscopy and quantitative tests for microbial growth assessment confirmed this observation. Concerning plate measurements, a device for plate reading on the surface of a whole 59 mm mat was used which allowed quantifying fluorescent stains on the surface of a electrospun mat. Fluorescent stains were used for the simultaneous identification of viable and non-viable cells. The results showed an increase in non-viable cells for 6 wt.% Co-SIM-1 mats of up to 40% for *P. putida*, with a parallel decrease in viable microorganisms. The effect was higher for *P. putida* than *S. aureus*, which could be associated with the different way of transporting cobalt in Gram-negative and Gram-positive bacteria. The comparison between the number of viable cells (FDA staining) and the number of CFU for cultures of *P. putida* and *S. aureus* showed a higher sensitivity of *P. putida* to the inclusion of cobalt in fibers with a reduction in the number of viable cells reaching 40% with respect to neat PLA mats. The results also showed higher relative FDA values with respect to CFU counting, which could be interpreted as a result of the existence of viable but non-culturable microorganisms (VBNC) associated to the inclusion of cobalt into fibers.

Acknowledgements

This work has been financed by the Dirección General de Universidades e Investigación de la Comunidad de Madrid, Research Network 0505/AMB-0395 and the Spanish Ministry of Science (CTM2013-45775).

Appendix A. Supplementary data

Supplementary data associated with this article can be found, in the online version, at http://dx.doi.org/10.1016/j.cej.2014.09.104.

References

[1] S. Kitagawa, R. Kitaura, S. Noro, Functional porous coordination polymers, Angew. Chem. Int. Ed., 43 (2004) 2334 –2375.

[2] L.J. Murray, M. Dincă, J.R. Long, Hydrogen storage in metal-organic frameworks, Chem. Soc. Rev., 38 (2009) 1294-314. 2

[3] L.R. MacGillivray, Metal-Organic Frameworks: Design and Application, Wiley, New York, 2010.

[4] L. Ma, C. Abney, W. Lin, Enantioselective catalysis with homochiral metal–organic frameworks, Chem. Soc. Rev., 38 (2009) 1248-1256.

[5] A.U. Czaja, N. Trukhan, U. Müller, Industrial applications of metal–organic frameworks, Chem. Soc. Rev., 38 (2009) 1284-1293.

[6] A.C. McKinlay, R.E. Morris, P. Horcajada, G. Férey, R. Gref, P. Couveur, C. Serre, BioMOFs: metal-organic frameworks for biological and medical applications, Angew. Chem., Int. Ed., 49 (2010) 6260-6266.

[7] S.M. Cohen, Postsynthetic methods for the functionalization of metal-organic frameworks, Chem. Rev. 112 (2012) 970-1000.

[8] M. Berchel, T. Le Gall, C. Denis, S. Le Hir, F. Quentel, C. Elleouet, T. Montier, J.M. Rueff, J.Y. Salauen, J.P. Haelters, G.B. Hix, P. Lehn, P.A. Jaffres, A silver-based metal–organic framework material as a 'reservoir' of bactericidal metal ions. New J. Chem. 35 (2011) 1000–1003.

[9] Y. Liu, X. Xu, Q. Xia, G. Yuan, Q. He, Y. Cui, Multiple topological isomerism of three-connected networks in silver-based metal–organoboron frameworks, Chem. Commun., 46 (2010) 2608-2610.

[10] K.M. Hindi, T.J. Siciliano, S. Durmus, M.J. Panzner, D.A. Medvetz, D.V. Reddy, L.A. Hogue, C.E. Hovis, J.K. Hilliard, R.J. Mallet, C.A. Tessier, C.L. Cannon, W.J. Youngs, Synthesis, stability, and antimicrobial studies of electronically tuned silver acetate N-heterocyclic carbenes. J. Med. Chem., 51 (2008) 1577-1583.

[11] T.V. Slenters, J.L. Sague, P.S. Brunetto, S. Zuber, A. Fleury, L. Mirolo, A.Y.. Robin, M. Meuwly, O. Gordon, R. Landmann, A.U. Daniels, K.M. Fromm, Of chains and rings: Synthetic strategies and theoretical investigations for tuning the structure of silver coordination compounds and their applications, Materials, 3 (2010) 3407-3429.

[12] J. Merlino, P. Kennedy, Resistance to the biocidal activity of silver in burn wound dressings–is it a problem? Microbiology Australia, 31 (2010) 168-170.

[13] F.A. Sheikh, N.A.M. Barakat, M.A. Kanjwal, A.A. Chaudhari, I.H, Jung, J.H. Lee, H.Y. Kim, Electrospun antimicrobial polyurethane nanofibers containing silver nanoparticles for biotechnological applications, Macromol. Res. 17 (2009) 688-696.

[14] Q. Shi, N. Vitchuli, J. Nowak, J. Noar, J.M. Caldwell, F. Breidt, M. Bourham, M. McCord, X. Zhang, One-step synthesis of silver nanoparticle-filled nylon 6 nanofibers and their antibacterial properties, J. Mater. Chem., 21 (2011) 10330-10335.

[15] A.M. Abdelgawad, S.M. Hudson, O.J Rojas, Antimicrobial wound dressing nanofiber mats from multicomponent (chitosan/silver-NPs/polyvinyl alcohol) systems, Carbohydrate Polym., 100 (2014) 166–178.

[16] S.J. Lee, D.N. Heo, J.H. Moon, W.K. Ko, J.B. Lee, M.S. Bae, S.W. Park, J.E. Kim, D.H. Lee, E.C. Kim, C.H. Lee, I.K. Kwon, Electrospun chitosan nanofibers with controlled levels of silver nanoparticles. Preparation, characterization and antibacterial activity, Carbohydrate Polym. 111 (2014) 530–537.

[17] S. Aguado, J. Quirós, J. Canivet, D. Farrusseng, K. Boltes, R. Rosal, Outstanding antibacterial activity of Cobalt imidazolate Metal-Organic Frameworks, Chemosphere, 113 (2004) 188-192.

[18] A. Alonso, X. Muñoz-Berbel, N. Vigués, J. Macanás, M. Muñoz, J. Mas, D.N. Muraviev, Characterization of fibrous polymer slver/cobalt nanocomposite with enhanced bactericide activity, Langmuir, 28 (2012) 783-790.

[19] W. Zhuang, D. Yuan, J.R. Li, Z. Luo, H.C. Zhou, S. Bashir, J. Liu. Highly potent bactericidal activity of porous metal–organic frameworks. Adv. Healthcare Mater. 1 (2012) 225–238.

[20] M.P.A. Sancet, M. Hanke, Z.B. Wang, S. Bauer, C. Azucena, H.K. Arslan, M. Heinle, H. Gliemann, C. Woll, A. Rosenhahn, Surface anchored metal-organic frameworks as stimulus responsive antifouling coatings, Biointerphases, 8 (2013) 29, doi:10.1186/1559-4106-8-29.

[21] D. Li, Y. Xia. Electrospinning of Nanofibers: Reinventing the Wheel? Adv. Mater., 16 (2004) 1151–1170.

[22] A. Greiner, J. Wendorff. Electrospinning: a fascinating method for the preparation of ultrathin fibers. Angew. Chem., Int. Ed., 46 (2007) 5670–5703

[23] R. Ostermann, J. Cravillon, C. Weidmann, M. Wiebcke, B.M. Smarsly, Metal-organic framework nanofibers via electrospinning. Chem. Commun. 47 (2011) 442-444.

[24] K. Abdelrazek, H. Fouad, T. Elsarnagawy, F.N. Almajhdi. preparation and characterization of electrospun PLGA/silver composite nanofibers for biomedical applications. Int J. Electrochem. Sci., 8 (2013) 3483-3493.

[25] A. Dasari, J. Quirós, B. Herrero, K. Boltes, E. García-Calvo, R. Rosal. Antifouling membranes prepared by electrospinning polylactic acid containing biocidal nanoparticles. J. Memb. Sci., 405-406 (2012) 134-140.

[26] A. Moriya, T. Maruyama, Y. Ohmukai, T. Sotani, H. Matsuyama. Preparation of poly(lactic acid) hollow fiber membranes via phase separation methods. J. Membr. Sci. 342 (2009) 307–312.

[27] S. Aguado, J. Canivet, D. Farrusseng. Facile shaping of an imidazolate-based MOF on ceramic beads for adsorption and catalytic applications. Chem. Commun. 46 (2010) 7999–8001.

[28] S. Aguado, J. Canivet, D. Farrusseng,. Engineering structured MOF at nano and macroscales for catalysis and separation. J. Mater. Chem. 21 (2011) 7582–7588.

[29] R. Banerjee, A. Phan, B. Wang, C. Knobler, H. Furukawa, M. O'Keeffe, O.M. Yaghi, High-throughput synthesis of zeolitic imidazolate frameworks and application to CO_2 capture. Science, 319 (2008) 939–943.

[30] A.J. Driscoll, N. Bhat, R.A. Karron, K.L. O'Brien, D.R. Murdoch. Disk diffusion bioassays for the detection of antibiotic activity in body fluids: applications for the pneumonia etiology research for child health Project. Clin. Infect. Dis. 54 (2012) S159-S164.

[31] B. Faure, G. Salazar-Alvarez, A. Ahniyaz, I. Villaluenga, G. Berriozabal, Y.R. de Miguel, L. Bergström, Dispersion and surface functionalization of oxide nanoparticles for transparent photocatalytic and UV-protecting coatings and sunscreens. Sci. Technol. Adv. Mater. 14 (2013) 023001.

[32] J. Huang, T. You, Electrospun Nanofibers: From Rational Design, Fabrication to Electrochemical Sensing Applications, in: R. Maguire (Ed.), Advances in Nanofibers, Intech Open, 2013, pp. 35-83.

[33] J.S. Baker, L.Y. Dudley. Biofouling in membrane systems. A review. Desalination 118 (1998) 81-90.

[34] S. Croes, R.H. Deurenberg, M.L. Boumans, P.S. Beisser, C. Neef, E.E. Stobberingh. *Staphylococcus aureus* biofilm formation at the physiologic glucose concentration depends on the *S. aureus* lineage. BMC Microbiology, 9 (2009) 229.

[35] L. Hall-Stoodley, J.W. Costerton, P. Stoodley. Bacterial biofilms: from the natural environment to infectious diseases. Nat. Rev. Microbiol. 2 (2004) 95-108.

[36] J.D. Oliver. The public health significance of viable but non-culturable bacteria, in R.R. Colwell and D.J. Grimes (Eds.), Nonculturable Microorganisms in the Environment. American Society for Microbiology Press, Washington D.C., 2000, pp. 277-299.

[37] D. Venieri, E. Chatzisymeon, M.S. Gonzalo, R. Rosal, D. Mantzavinos, Inactivation of *Enterococcus faecalis* by TiO_2 -mediated UV and solar irradiation in water and wastewater: culture techniques never say the whole truth, Photochem. Photobiol. Sci. 10 (2011) 1744-1750.

[38] D.H. Nies. Microbial heavy-metal resistance. Appl. Microbiol. Biotechnol. 51 (1999) 730-750.

[39] J. Horowitz, M.D. Normand, M.G. Corradini, M.Peleg. Probabilistic model of microbial cell growth, division, and mortality. Appl. Environ. Microbiol. 76 (2010) 1 230-242.

Supplementary information

Antimicrobial metal-organic frameworks incorporated into electrospun fibers

Jennifer Quirós[a], Karina Boltes[a], Sonia Aguado[a], Roberto Guzman de Villoria[b], Juan José Vilatela[b] and Roberto Rosal[a,c,*]

[a] Department of Chemical Engineering, University of Alcalá, 28871 Alcalá de Henares, Madrid, Spain
[b] Madrid Institute for Advanced Studies of Materials (IMDEA Materials Institute), Tecnogetafe, E-28906, Madrid, Spain
[c] Madrid Institute for Advanced Studies of Water (IMDEA Agua), Parque Científico Tecnológico, E-28805, Alcalá de Henares, Madrid, Spain

Contents:

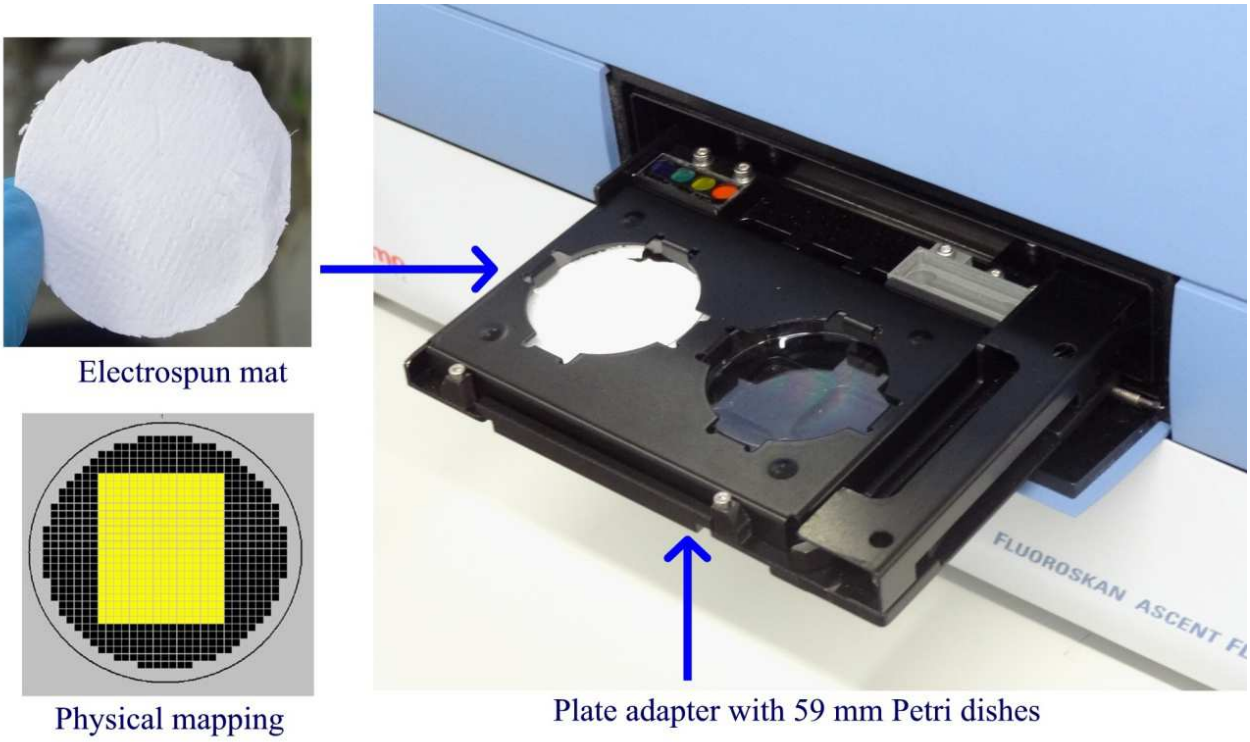

Fig. S1. Detail of membrane holder for fluorescence measurements using an adapted plate reader. The measurement gives 20 x 16 data points indicated in yellow.

* corresponding author: roberto.rosal@uah.es

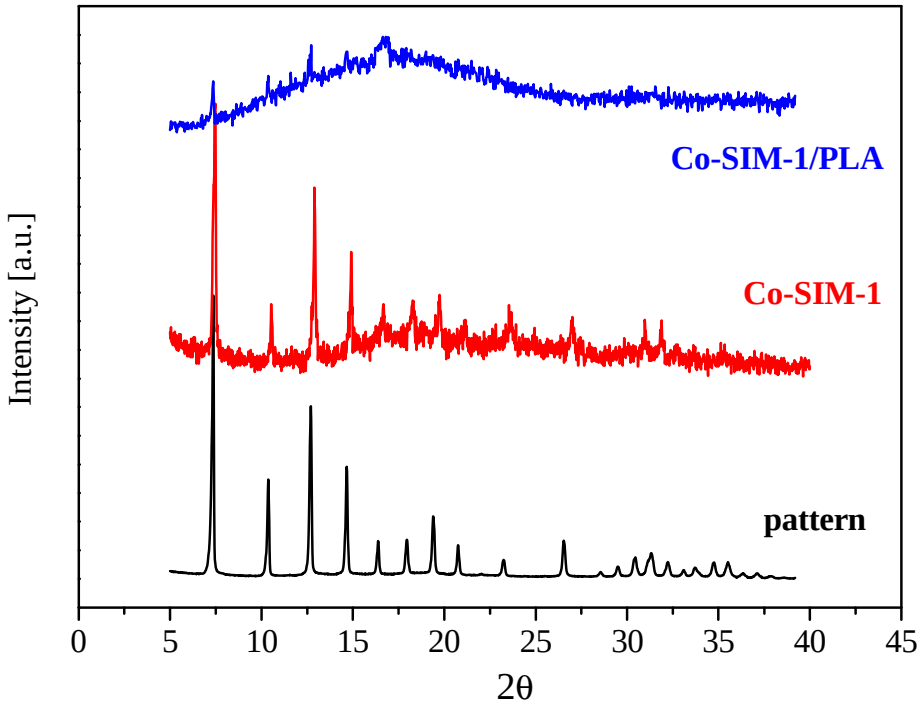

Fig. S2. XRD pattern of Co-SIM-1.

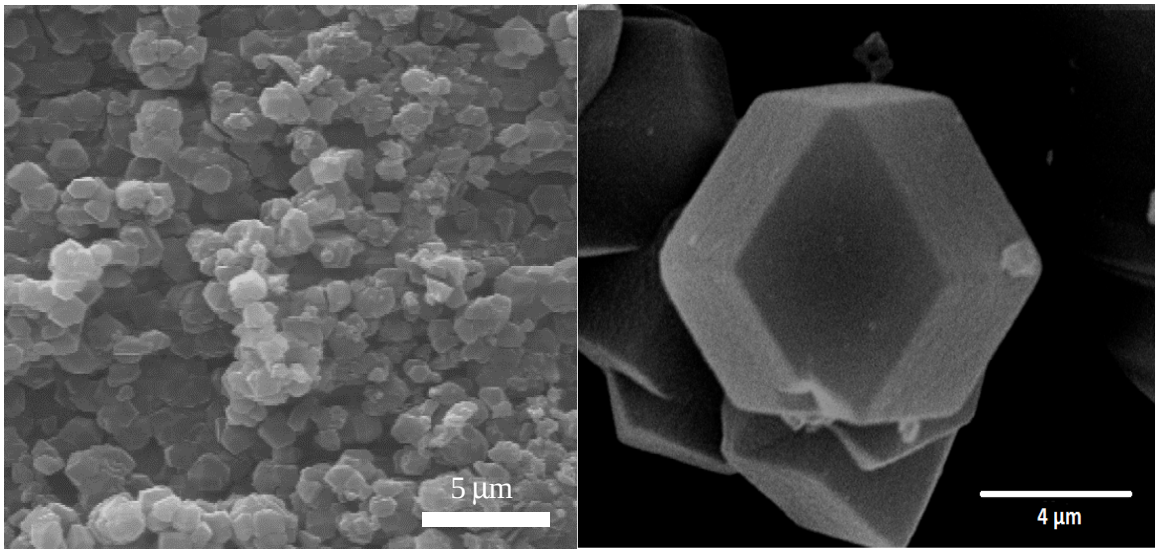

Fig. S3. SEM micrographs of Co-SIM-1 particles. Left: detail of a larger particle.

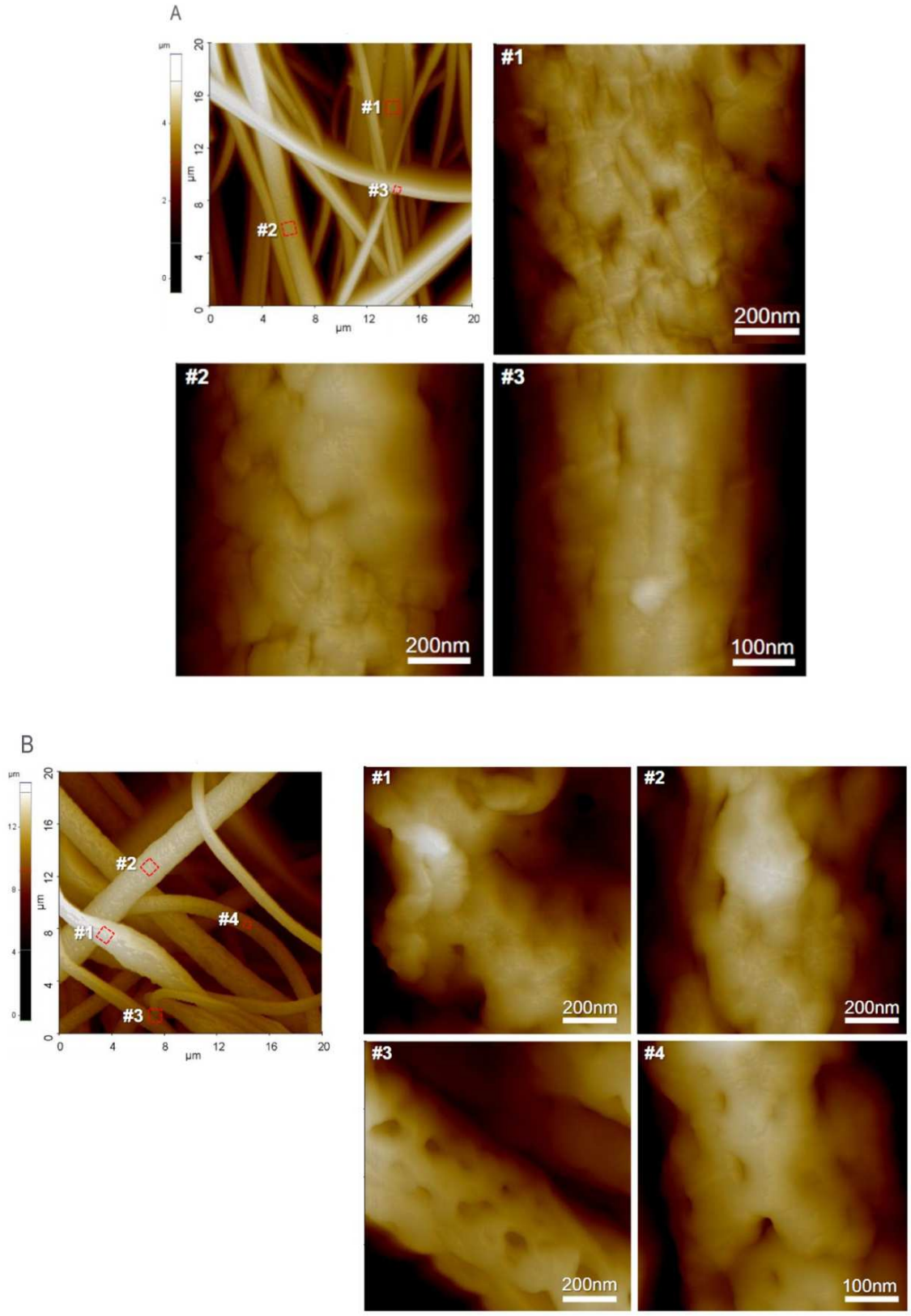

Fig. S4. AFM images of net PLA (A) and Co-SIM-1 loaded PLA fibers (B).

A

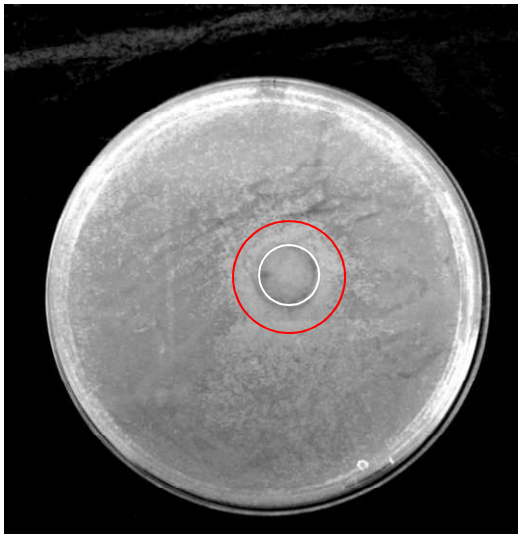

B

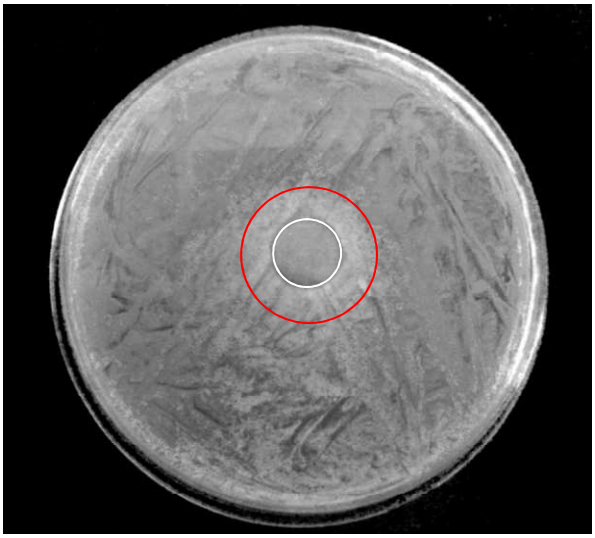

Fig. S5. Disk diffusion experiment to estimate antibacterial activity on (A) *P. putida* and (B) *S. aureus*. The circles indicate inhibition areas.